coatings

MDPI

Article

A Novel Protection Method for Carbonate Stone Artifacts with Gypsum Weathering Crusts

Ruicong Lu [1,2,3], Lu He [1,2,3], Ting Li [1,2,3], Fuwei Yang [1,2,3,*], Yan Liu [1,2,3], Kun Zhang [1,2,3] and Xinnan Chen [1,2,3]

[1] China-Central Asia "the Belt and Road" Joint Laboratory on Human and Environment Research, Northwest University, Xi'an 710127, China
[2] Key Laboratory of Cultural Heritage Research and Conservation, Northwest University, Xi'an 710127, China
[3] School of Culture Heritage, Northwest University, Xi'an 710127, China
* Correspondence: yangfuwei@nwu.edu.cn

Abstract: An innovative method using a methanol solution of barium hydroxide-urea as a protective agent was investigated for the conservation of stone artifacts with harmful gypsum weathering crusts. In this method, the methanol solution of barium hydroxide-urea and water were introduced into the gypsum crust in sequence by surface spraying. By doing so, the harmful gypsum crust is directly converted into a barium sulfate—calcium carbonate composite protective layer. The properties of the composite layer were characterized by SEM-EDX, XRD, ATR-FTIR, IC, water solubility, wetting angle, color difference, open porosity, capillary water absorption, and surface hardness. The results of the morphological and composition characterization (SEM-EDX, XRD, ATR-FTIR) indicate that the added urea can promote the carbonization reaction effectively. In addition, the methanol solution of barium hydroxide-urea can penetrate deep into the gypsum crust. The results of the physical properties characterization denote that the water stability of the specimens was significantly increased after the protection treatment; an approximate ten-fold stronger water resistance ability was achieved. Meanwhile, the intrinsic physical properties of gypsum crust, such as pore structure and original appearance, could basically be maintained. The presented conservative method has high facility and controllability and satisfying conservation effect, which means it has potential in the conservation of surface weathering carbonate stone artifacts.

Keywords: barium hydroxide; urea; methanol solution; gypsum crust; stone artifacts

Citation: Lu, R.; He, L.; Li, T.; Yang, F.; Liu, Y.; Zhang, K.; Chen, X. A Novel Protection Method for Carbonate Stone Artifacts with Gypsum Weathering Crusts. *Coatings* **2022**, *12*, 1793. https://doi.org/10.3390/coatings12111793

Academic Editor: Enrico Quagliarini

Received: 10 October 2022
Accepted: 18 November 2022
Published: 21 November 2022

1. Introduction

Calcareous stone artifacts are widespread around the world. However, the stability of such artifacts is not strong enough [1,2]. As a result, they are susceptible to corrosion, and weathering diseases are prevalent among them. There are a number of factors that can cause this damage, and the effects of sulfur oxides are non-negligible. With the development of industrialization, the contents of these kinds of chemicals have increased dramatically and will react with the calcareous stone artifacts [3]. This will transform calcium carbonate into calcium sulfate, which will eventually generate the gypsum crust [4]. The resulting gypsum crust is believed to be one of the most destructive weathering products for contaminated artifacts. This mainly results from the much higher solubility of gypsum in water ($Ksp = 3.14 \times 10^{-5}$) than that of calcium carbonate ($Ksp = 3.36 \times 10^{-9}$) [5]. Thus, the surface erosion of stone artifacts with gypsum weathering crusts can be readily caused by rain scouring. In addition, the higher solubility of gypsum can lead to serious flaking and crumbling damage of the stone artifacts because of the re-crystallization pressure [6,7].

Different types of methods have been studied to conserve the stone artifacts, and several new approaches have been proposed in recent years. Removing the gypsum crust directly via cleaning is a traditional method and various techniques have been investigated by

scientists, such as laser cleaning, chemical cleaning, and bio-cleaning [8–10]. Recently, Yan Liu et al. (2021) put forward a novel method using the scavenger of barium carbonate embedded in an absorbent cotton-coating; they let it react with the calcium sulfate specifically to achieve a targeted cleaning outcome on a surface sulfated marble [11]. Cleaning is an effective method. However, in most cases, the surfaces of the stone artifacts always contain different decorative elements or characteristics that carry important historical and cultural data [12]. Therefore, since the losses of historical and cultural values are irreversible, the gypsum crust cannot be simply removed in its entirety. With the development of organic materials, they have been applied in many areas, including the conservation of deteriorated stone artifacts. Commercial acrylic and methacrylic resins have been extensively applied since the 1960s [13]. However, these conventional organic polymers are incompatible with the inorganic substrates protected and show distinct aging phenomena, such as yellowing, cracking, and embrittlement after a period of time [14]. In recent years, inorganic components have been added to improve the properties of pure organic polymers. Many different kinds of inorganic nanometric reinforcing agents, such as TiO_2 and SiO_2, were incorporated with organic polymers by scientists who sought better conservation material [15]. Nevertheless, recent results showed that the added TiO_2 nanoparticles can cause the degradation of the incorporated Paraloid B-72 after exposure to UV light for a certain period of time; other outcomes also indicate that the durability of these organic–inorganic hybrid materials are not satisfying [16]. Conversely, the inorganic materials show high compatibility with the protected inorganic substrates; thus, leading to high durability. Lime water and barium hydroxide aqueous solution were the earliest-studied inorganic consolidants [17]. Nevertheless, their conservation effects are also dissatisfactory. The use of lime water was previously estimated to be inefficient, mainly due to the low solubility of calcium hydroxide in the water. Even with a massive amount of time of the conservation treatment, the obtained conservation effect is still very poor [18]. Theoretically, the barium hydroxide aqueous solution can convert the hazardous gypsum crust into barium sulfate and calcium hydroxide, which could gradually be carbonized to calcium carbonate. These acquired substances will provide protective effects against the decay of the stone [17]. Nonetheless, the extremely high reactivity of barium hydroxide in an aqueous solution makes this material unsatisfactory. When it contacts carbon dioxide in the atmosphere and the gypsum (or another sulfate, such as sodium sulfate in the interior of the stone artifacts), barium carbonate, barium sulfate, calcium hydroxide, as well as other chemicals would yield rapidly [19]. These substances will hinder the barium hydroxide aqueous solution from deeper penetration into the substrate, leading to a relatively restricted conservative effect presented only on the very surface of the substrate rather than providing sustained effective protection [20]. Hence, the Ferroni–Dini method was developed to obtain better conservation results. This method consists of two sequential procedures: desulfuration by a solution of ammonium carbonate and consolidation by an aqueous solution of barium hydroxide. The added desulfuration procedure aims to reduce the amount of the sulfate on the surface of the infected cultural heritage to ensure the better ability of the barium hydroxide aqueous solution to penetrate deep into the substrate and obtain a better conservation effect [21]. However, after this treatment, different outcomes occur on different kinds of cultural heritages. It achieves positive results on the frescoes and, inversely, negative consequences on the stone artifacts [22,23]. The reason for this should be that the gypsum crust on frescoes is thin and could obtain complete desulfuration [24]. On the contrary, the gypsum crust on stone artifacts is too thick to obtain complete desulfuration [25]. Therefore, the undesired reactions mentioned above will inevitably occur on stone artifacts with gypsum weathering crusts and lead to unsatisfactory protective properties. Thus, some new kinds of inorganic materials have also recently been explored, such as hydroxyapatite, nano calcium hydroxide, and barium hydroxide dispersions [26,27]. Nevertheless, the shortcomings of these materials are also evident. The introduction of hydroxyapatite would provide an abundant source of phosphorus in favor of many microorganisms. As for the nano organic materials, the

preparation methods are mostly complicated [28]. In addition, nanoparticles tend to agglomerate; this will constrain their penetrability. Hence, the conservation effect can be impaired, too.

With all the limitations of the materials mentioned above, recently, we proposed the methanol solution of barium hydroxide as a novel treatment agent for the conservation of stone artifacts with gypsum weathering crust; the results were satisfying because of the organic solvent employed. When barium hydroxide is dissolved in a methanol solvent, it does not possess the activity to react with carbon dioxide in the atmosphere and calcium sulfate in the gypsum crust, as they are ionic reactions that can only occur in aqueous solutions. As a result, insoluble substances, i.e., barium carbonate, barium sulfate, and calcium carbonate, are not produced, ensuring that the solution has the ability to penetrate deep into the substrate. Moreover, the solubility of the barium hydroxide in the methanol solvent is much higher and the preparation method of the new treating solution is fairly facilitated [29]. However, this approach may face obstacles when applied to outdoor calcareous stone artifacts due to difficulties in further carbonating the resulting calcium hydroxide. Because the methanol solution of barium hydroxide can delve deep into the substrate, the carbonization reaction of the calcium hydroxide produced in the inner part of the substrate could be restricted since the content of the carbon dioxide in the atmosphere is quite low (0.038%) and the surface reaction will take place first. Thus, the complete carbonation reaction of outdoor stone artifacts after treatment with a barium hydroxide methanol solution may take a long time. Hence, in this paper, we prepare a methanol solution of barium hydroxide-urea as a new reagent for the conservation of stone artifacts with gypsum weathering crusts. The addition of urea could provide a continuous source of carbonate ions and permit a continuous carbonation reaction without compromising the advantages of the barium hydroxide methanol solution. Therefore, the ability of the methanol solution of barium hydroxide-urea to penetrate deep into the gypsum crust, as well as the high controllability (the reaction only occurs after the water supply) of this application strategy, will be maintained; they are of great importance for the conservation of stone artifacts with gypsum weathering crusts. In addition, due to the addition of urea, the entire conservation reaction can take place from the interior of the substrate without restriction, and the unstable intermediate product calcium hydroxide will be eliminated as soon as possible. Hence, a good conservation effect will be ensured. In application, the methanol solution of barium hydroxide-urea was first applied into the gypsum crust at different times to compare the conservation effects of the different amounts of introduced protectants. Water was then provided to stimulate reactions between them. The simple application procedures of the proposed protectants are shown in Figure 1. The conservation effect was evaluated by SEM-EDX, XRD, ATR-FTIR, water solubility, color difference, IC, wetting angle, open porosity, capillary water absorption, and surface hardness.

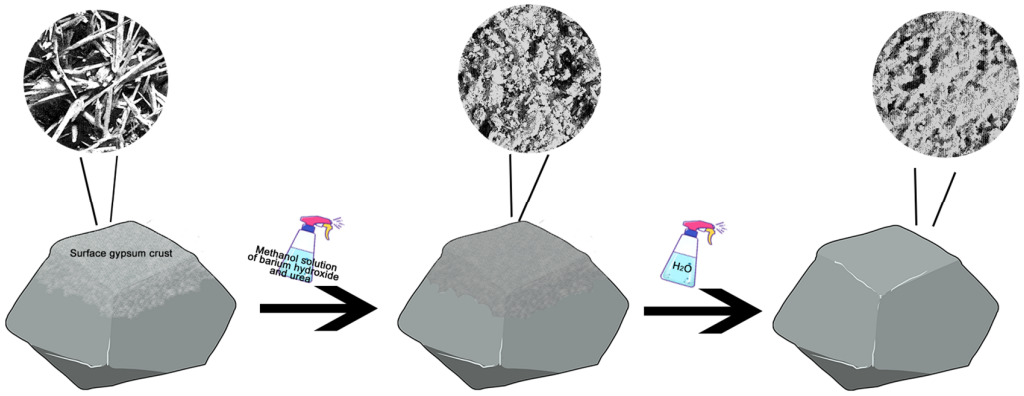

Figure 1. Conservation schematic diagram of surface gypsification stone artifacts.

2. Materials and Methods

2.1. Sample Preparation

All chemicals were of analytical grade and used without further purification. $Ba(OH)_2$, urea, and anhydrous methanol were purchased from Sinopharm Group Co., Ltd., Shanghai, China.

Referring to the previous literature, the specimens were prepared by the following method: the marble specimens (2.0 × 2.0 × 2.0 cm) were cleaned with deionized water first and then left to dry for one day. Afterward, to simulate a surface gypsum crust, the specimens were placed into an aqueous solution of H_2SO_4 at pH 2 for 24 h [26]. Then, the specimens were taken out and further desiccated prior to use.

The mixed solution of barium hydroxide-urea in methanol at a concentration of 10% was prepared by dissolving barium hydroxide and urea into the anhydrous methanol. After stirring for hours, the solution was centrifuged and ready for use.

The conservation routine was as follows: the specimens were sprayed with the reagent solution until they could no longer be absorbed and then left to dry in a confined environment. In order to compare the conservation effects of the different amounts of introduced protectants, the above operation was operated three successive times on three sets of specimens, each containing five specimens. Later, the specimens were provided with sufficient water by spraying, and further cured for one month in a sealed and moist environment before various tests were carried out. The protective performances of the specimens with different numbers of treatments were characterized by water solubility, color difference, IC, wetting angle, open porosity, capillary water absorption, and surface hardness. To further characterize the conversion process of the conservation treatment, SEM, XRD, and FTIR were performed on 3-fold-treated specimens, from which the best conservation effects were obtained.

2.2. Characterization

The structure and composition of the specimens were analyzed by scanning electron microscopy (SEM, VEGA-3XMU, TESCAN, Brno, Czech, BSE mode, 12.00 kV of accelerating voltage, and 10.0 mm of working distance) with energy-dispersive X-ray spectroscopy (EDX, Genesis 2000 XMS, EDAX, Inc., Mahwah, NJ, USA), X-ray diffractometry (XRD, Smart Lab, Rigaku, Tokyo, Japan, Cu Ka radiation, scanning range 10°~90°, step length 0.01°, scanning speed 10°/min), and attenuated total reflectance–Fourier transform infrared (ATR-FTIR, TENSOR 27, Bruker, Billerica, MA, USA, scanning wave number 4000–600 cm^{-1}, resolution 4 cm^{-1}, scanning times 16 times) spectroscopy.

The water solubility of the specimens with different times of the conservation treatment was approximately measured by a conductivity meter (DDSJ-308F, Rex, INESA Scientific Instrument Co., Ltd., Shanghai, China). The specimens were placed in a beaker containing 200 mL of water under mechanical agitation, and the conductivity values of the solution were recorded automatically every minutes as soon as the specimens were placed in the beaker until the values were approximately steady. Ion chromatography (IC, ICS 1100/1600, Thermo Fisher Scientific, Cleveland, OH, USA) was applied to further affirm the ion content of the solution after the detection of the water solubility of the specimens.

To assesses the water repellency of the specimens, the wetting angles of the specimens were tested via a contact angle tester (JGW-360B, Beijing Haifuda Technology Co., Ltd., Beijing, China).

To evaluate the color differences of the specimens, a portable colorimeter (WSC-2B, INESA Scientific Instrument Co., Ltd., Shanghai, China) was used. The treated specimens after curation were further desiccated under dry and ventilated conditions for 3 days and were then tested. Five points from the different parts of the surfaces of each blank and treated specimen were tested to minimize the experimental error. The results were analyzed according to the colorimetric coordinates (CIELAB); the formula is as follows:

$$\Delta E^* = (\Delta L^{*2} + \Delta a^{*2} + \Delta b^{*2})^{1/2} \quad (1)$$

According to this color representation, L* is lightness, a* is the red–green component, and b* is the yellow–blue component [30].

To determine the capillary water absorption and open porosity of the specimens, an electronic density tester (MZ-C300, Mayzun, Shenzhen, China) was employed.

To invest in the surface hardness of the specimens, a shore D durometer (LX-D-1, Dongguan SanLiang measuring tools Co., Ltd., Dongguan, China) was applied.

3. Results and Discussion

3.1. Morphological and Chemical Characterization

The surface microstructure changes of the specimens are shown in Figure 2. As expected, a loosened needle-like morphology appeared for the blank specimen (Figure 2a,d). The micropores are clearly visible, as depicted in Figure 2d. This typical gypsum morphology has been confirmed by many scientists before [31,32]. The characteristic diffraction peaks (d = 7.6057, 4.2649, 3.7912, 3.0515, 2.8643, 2.6760 Å) in the XRD results (Figure 3a) further corroborated the gypsum component. After introducing only the methanol solution of barium hydroxide-urea, it can be seen in Figure 2e that the labeled in-compact protectants scattered across the entire surface act similarly to padding rather than provide any connection strength. The voids and pores of the original blank specimens were completely covered by them (Figure 2b,e). For the XRD results, gypsum is still the only phase that could be observed and the existence of the barium-contained phases could not be detected (Figure 3b). The reason for this could be that the barium-containing phases were in amorphous form and the XRD representation was not able to identify these types of entities. This denotes that the reaction between the reagent solution and the gypsum crust will not occur without the water supply. This is because the reactions between them are ionic and cannot occur in organic solvents. After the supply of water, however, there was an evident change in the morphology of the treated specimens. The in-compact padding substance before the water supply changed into a more continuous structure. The scattered introduced conservative materials and the original gypsum matrix merged entirely (Figure 2c,f). The XRD results further reveal that the compositions of the newly emerged structure are barium sulfate (d = 3.8898, 3.4333, 3.3106, 2.8376, 2.1008 Å) and calcium carbonate (d = 3.0362, 2.2847, 1.9111, 1.8748 Å) (Figure 3c). Thus, the new compact structure presented in Figure 2c,f is a barium sulfate-calcium carbonate composite layer. In addition, the crystallographic form of the calcium carbonate is calcite; this follows the investigation results of the previous studies, i.e., the addition of water supply is more likely to produce calcite. On the contrary, when there is a large number of organic molecules in the solution and no straight water supply, this shows a tendency to favor the formation and kinetic stabilization of vaterite instead of stable calcite [33,34]. These results indicate that the conservation reaction between barium hydroxide and the gypsum crust is completed after the water supply. Because of the introduction of water, the urea was decomposed into the form of ammonia and carbon dioxide. The ammonia was released into the environment; the carbon dioxide produced via this process was performed as a continuous source of carbonate ions to lead to the carbonation reaction from the internal substrate. The chemical equations are as follows:

$$CO(NH_2)_2 + H_2O = CO_2 + 2NH_3 \quad (2)$$

$$Ba(OH)_2 + CaSO_4 = BaSO_4 + Ca(OH)_2, \quad (3)$$

$$Ca(OH)_2 + CO_2 = CaCO_3 + H_2O \quad (4)$$

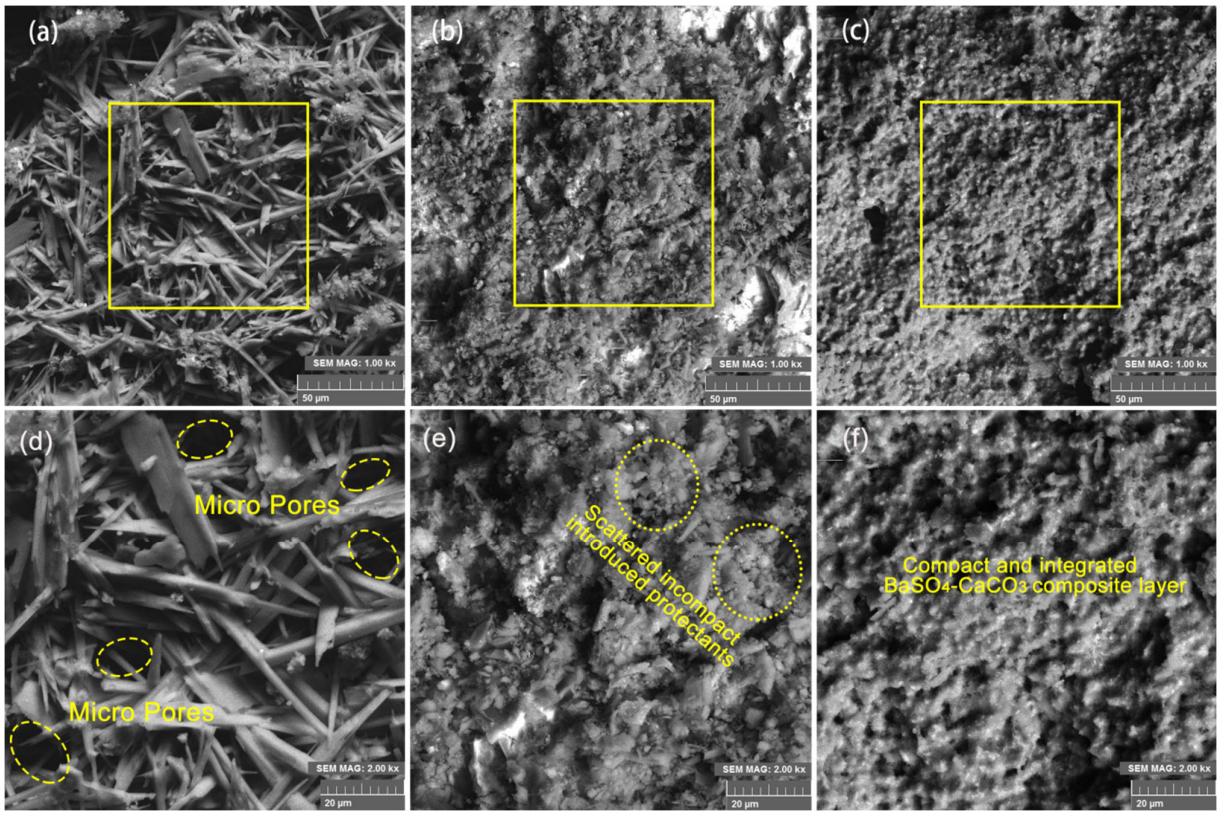

Figure 2. Surface morphology of the specimens with different magnifications (the yellow rectangle areas of the (**a**–**c**) are magnified to (**d**–**f**), respectively), (**a**,**d**): blank specimen, (**b**,**e**): treated specimen before water supply, (**c**,**f**): treated specimen after water supply.

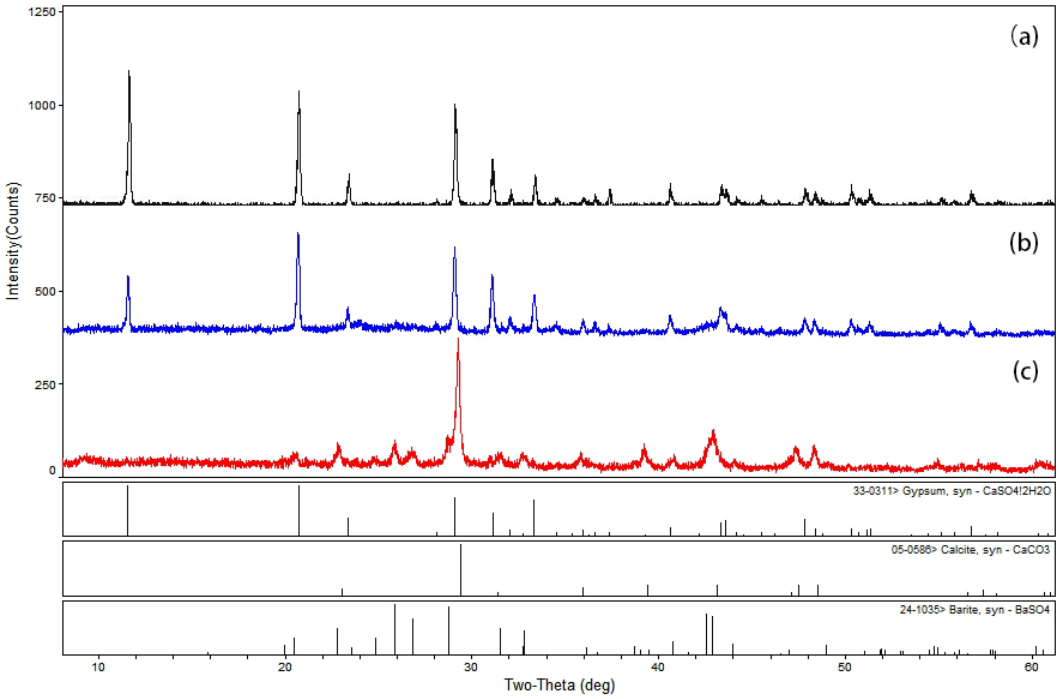

Figure 3. XRD results of the specimens: (**a**) blank specimen, (**b**) treated specimen before water supply, (**c**) treated specimen after water supply.

The FTIR spectra of the specimen after treatment with the reagent solution and before the water supply are presented in Figure 4. Moreover, the spectra of the gypsum, barium hydroxide, and urea are displayed for comparison. As shown in Figure 4, the characteristic peaks of the gypsum matrix can be clearly observed from the spectrum of the specimen. The general trend of peaks around 2250 cm^{-1} and 2800 cm^{-1} in the spectrum of the specimen is consistent with the spectrum of barium hydroxide, suggesting the presence of barium hydroxide. Meanwhile, the absence of the sharp vibrational band of OH stretching modes in $Ba(OH)_2$ located at 3570 cm^{-1} in the specimen's spectrum should be attributed to the reaction between barium hydroxide and methanol [35,36]. The peaks that appeared at around 1620 and 1460 cm^{-1} can be assigned to amide II bending and C-N stretching vibrations of the urea [37]. In addition to the peaks mentioned above, other peaks are marked in the figure and can further confirm the successful introduction of barium hydroxide and urea into the specimen, which cannot be verified in the XRD results. The FTIR results for the specimen after the water supply are depicted in Figure 5. Similar to Figure 4, the spectra of the potential (definite) components of the specimen are also presented. Even though the spectra of the calcite and barium carbonate are highly similar, the sharp peaks located at 1797, 874, and 711 cm^{-1} in the spectrum of the specimen can easily be attributed to calcite, as their specific locations are quite different from those of the barium carbonate peaks. However, the peak for mode v_3 of the CO_3^{2-} is located at 1454 cm^{-1} in the specimen's spectrum, which is slightly different from the spectrum of the calcite. Nevertheless, the slight discrepancy of this peak is not crucial for the confirmation of the calcite as it can shift occasionally; this can also be observed in the other forms of calcium carbonate. Conversely, the peaks of the other forms of the calcium carbonate located at lower wavenumbers, such as calcite (874 and 711 cm^{-1}), aragonite (856 and 711 cm^{-1}), and vaterite (875 and 745 cm^{-1}), are usually not changed under different situations [33,38–40]. Hence, the existence of the calcite can be fully ascertained here; this is in accordance with the XRD results. The appearance of the peaks at 637 and 610 cm^{-1} in the spectrum of the specimen, when compared with that of the gypsum, should certainly be ascribed to barium sulfate. In addition, the absorption peaks at 1080 cm^{-1} in the specimen's spectrum come from the sulfur-oxygen (S-O) stretching of the barium sulfate [41]. These FTIR analytical data are in good agreement with the XRD results and can further complete the results. In the XRD results, the urea and barium hydroxide cannot be distinguished from the spectrum before the water supply. Nevertheless, these substances can be clearly identified from the FTIR results. Therefore, the whole reaction process is fully confirmed.

To determine the length of time required for the conservation reaction to occur entirely, the FTIR was applied to identify the extent of the reaction since the reagent solution was introduced and the spectra are shown in Figure 6. For FTIR spectra, the quantitative analysis of different substances in the tested specimen was normally performed by comparing peak intensities. Hence, herein, the peak intensities of the characteristic peaks of the produced calcium carbonate (1454, 874 cm^{-1}) and barium sulfate (1080 cm^{-1}) can be used to ascertain the contents of them in the treated specimen and estimate the extent of the conservation reaction. By comparing the peak intensities of the calcium carbonate (874 cm^{-1}) and original gypsum crust (668 cm^{-1}), it is evident in Figure 6 that the peak intensity of calcium carbonate shows an incremental trend along with the time; however, it started barely to change after 4 days of the water supply. Meanwhile, the peak intensity of the barium sulfate (1080 cm^{-1}) also presented the same accumulative trending as that of calcium carbonate, which can be observed in Figure 6. In addition, the intensity of the peak located at 1454 cm^{-1} for the calcium carbonate almost did not alter at different times; this was observed in the preceding studies [40,42]. However, as depicted in Figure 6, the lengths of the vertical red lines may also stand for the content of the calcium carbonate. This is because the spectrum of the pure calcium carbonate shows a distinct downward feature at around 1400 cm^{-1} (Figure 5). The lengths of the red lines indicate the extent of this downward feature, which is the content of the calcium carbonate. It also increases

during the first four days after the water supply and is almost unaltered thereafter. Therefore, the whole conservation reaction can take place within one week.

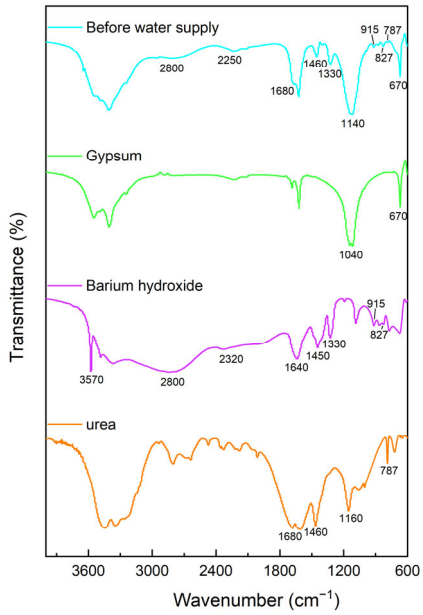

Figure 4. FTIR spectra of the specimen before the water supply.

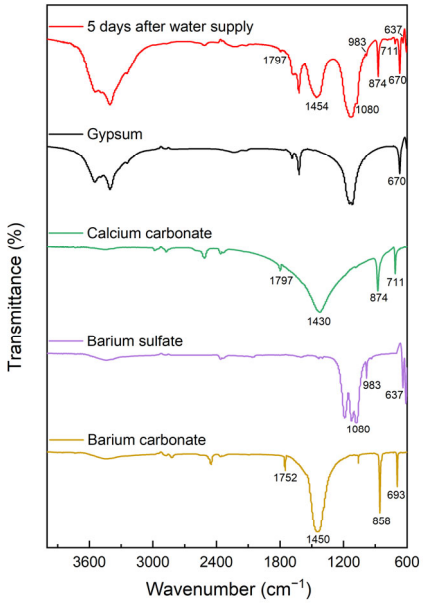

Figure 5. FTIR spectra of the specimen after the water supply.

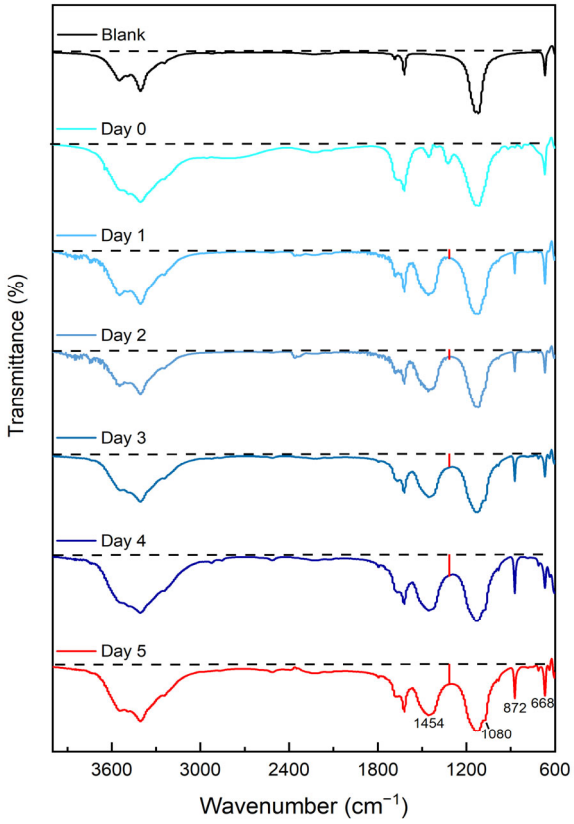

Figure 6. FTIR spectra of the specimens at different time intervals.

The cross-sectional morphology changes of the specimens are shown in Figure 7. The blank specimen displays a structure in agreement with the surface morphology (Figure 7a,d). After being treated with a reagent solution, and before being supplied with water, the morphology of the specimen showed a difference. As labeled in Figure 7e, the areas represented by the five yellow lines are a little darker than their surrounding areas and there are other different parts similar to them. In addition, the surrounding areas in lighter colors show cobweb-like morphology. It is clear that these features are not presented in the blank specimen and it should be the result from the introduced protectants. The surrounding areas in lighter colors should be the introduced protectants that cover the original gypsum substrate. However, the specimens need to be broken to observe the cross-sectional morphology. Through this process, the original morphology of the specimens can be affected. The gypsum substrate, which is supposed to be covered evenly, is partially exposed, and the exposed gypsum substrates can be observed as the darker areas labeled in Figure 7e. After the water was provided, a more compact structure emerged, and the gypsum substrate was hardly exposed (Figure 7c,f). The needle-like structure of the blank specimen is tightly folded by the newly produced material, which is barium sulfate and calcium carbonate according to the aforementioned XRD and FTIR results. The EDX results of the treated specimens before and after the water supply indicate that the reagent solution has the ability to penetrate deep into the substrate. The even distribution of the barium element can be detected consistently from the surface to a depth of about 3000 μm for the specimen provided with water (Figure 8right), which is a little deeper than the specimen before the water supply (Figure 8left). This may be due to some protective materials being transferred with the flowing water. These results imply that the ability of the methanol solution of barium hydroxide to penetrate deep into the substrate

was not affected by the adding urea and it is still much better than the aqueous solution because of the organic solvent adopted [29].

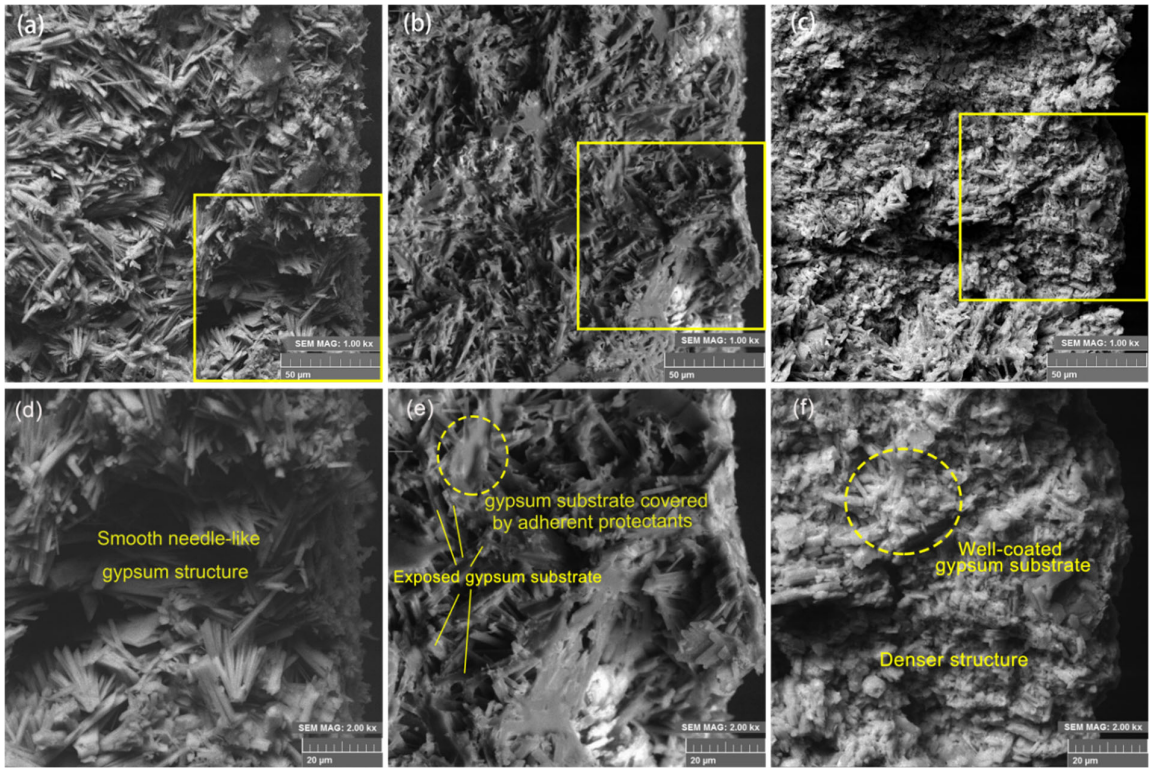

Figure 7. Cross-section morphology of the specimens with different magnifications (the yellow rectangle areas of the (**a**–**c**) are magnified to (**d**–**f**), respectively), (**a**,**d**): blank specimen, (**b**,**e**): treated specimen before water supply, (**c**,**f**): treated specimen after water supply.

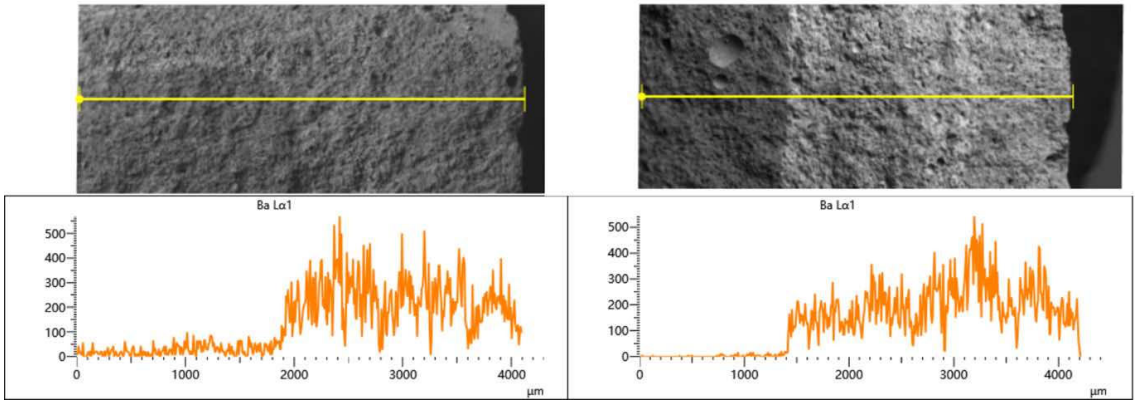

Figure 8. Line scan results of specimens; (**left**): the treated specimen before water supply, ((**upper**): SEM image with the yellow line analyzed by EDX, (**lower**): line scan results of the barium element), (**right**): treated specimen after water supply, ((**upper**): SEM image with the yellow line analyzed by EDX, (**lower**): line scan results of the barium element).

3.2. Physical Properties Characterization

Electrical conductivity was used to evaluate the water solubility of the specimens; the results are illustrated in Figure 9. It is commonly used for indicating the total concentration of the ionized constituents of a solution and is positively related to the sum of the anions (or cations) chemically determined [43]. Gypsum is a fairly dissoluble salt. Hence,

when the blank specimen was placed into the water, an appreciable quantity of the gypsum was decomposed into calcium ions and sulfate ions, which made the electrical conductivity of the blank specimen reach about 1800 μS/cm. After the conservation operation, the less soluble barium sulfate and calcium carbonate will be produced and the original gypsum substrate will be covered, according to the SEM images. Thus, the conductivity of the treated specimens is significantly reduced. The maximum value of the conductivity of the specimen with only one spray operation is about 800 μS/cm and it could be further decreased to about 500 μS/cm after two operations. After triple-spray operations, the value is only about 250 μS/cm, which is far below the results of the blank specimen. The most likely causes for these different degressive results are that the barium hydroxide absorbed by the specimens (with different spray-operation times) is incremental and the gypsum substrate could be coated better.

The IC results are delineated in Figure 10 and the specific data values are exhibited in Table 1. Due to instrumental limitations, SO_4^{2-} is the only ionic species that can be efficiently detected and is relevant to this study. In general, the regularity of the variation of the SO_4^{2-} content among the different solutions is roughly consistent with the conductivity results. The solution of the blank specimen reaches its highest value and the solution of the specimen after three treatments achieves its lowest, as expected. As mentioned above, due to the difference in solubility between the original substrate gypsum and the product barium sulfate, the SO_4^{2-} in the solution should mainly originate from the gypsum. In addition, the SO_4^{2-} content ratio between the blank specimen and the specimen after 3 treatments is as high as 30 (Table 1). This is a larger number compared with the approximate 8 times calculated from the electrical conductivity results. The reason for this could be that there may be some contamination ions in the specimens or the urea was not decomposed completely. Furthermore, the produced calcium carbonate may also have led to this outcome. This significant reduction in SO_4^{2-} content indicates that the initially susceptible gypsum crust was almost fully shielded after three treatments with the methanol solution of barium hydroxide and urea.

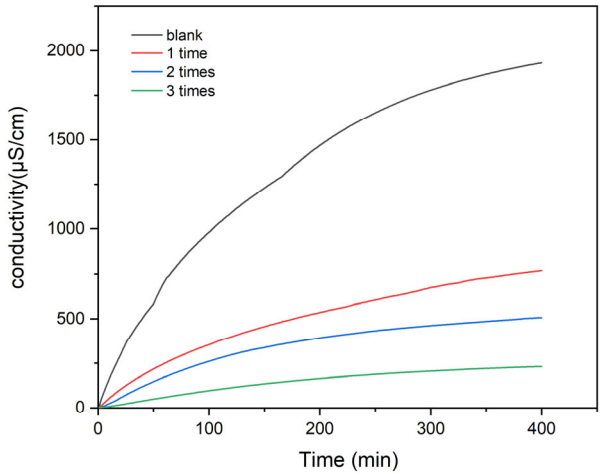

Figure 9. Conductivity results of the specimens before and after treatment.

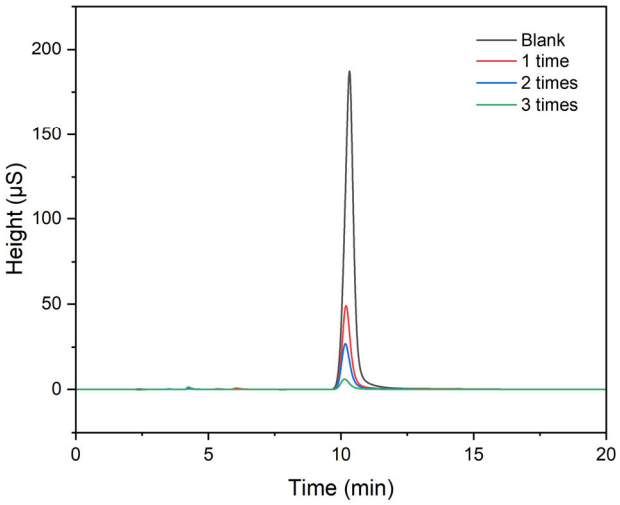

Figure 10. Ion chromatography results of the specimens before and after treatment.

Table 1. The SO_4^{2-} ion content of the specimens with different treatment numbers.

Specimens with Different Treatment Numbers	Type	Area (S*min)	Height (S)	Amount (mg/L)
0 (blank)	BMB	75.083	186.735	65.413
1	BMB	19.226	48.921	16.783
2	BMB	10.940	27.031	9.569
3	BMB	2.575	5.929	2.287

The outcomes of the wetting angles are displayed in Figure 11. All images were taken as soon as the droplets contacted the surface due to the high hydrophobicity of the gypsum substrate, after which, they were absorbed by the substrate. The wetting angle of the blank specimen was only 17.00° and increased slightly to 18.68° after being treated only once with the methanol solution of barium hydroxide and urea. After being treated twice, the wetting angle of the specimen changed to 30.00° and increased to 42.56° after three treatments. Typically, the magnitude of the wetting angle represents the hydrophilic or hydrophobic nature of the material. When the wetting angle of the surface is located in the range of 0° to 90°, the surface can be regarded as hydrophilic. Hence, the conservation treatment does not alter the hydrophilic nature of the original gypsum crust and the "breathing function" of the matrix could be maintained. The results show distinct differences with the organic coatings, which lead to a complete water repellency and are incompatible with the inorganic gypsum. Hence, this will eventually cause fissures and cracks [44,45]. However, despite the definition mentioned above, a larger wetting angle also represents a more hydrophobic surface even if it is an acute angle. Therefore, the surface of the specimen will become more hydrophobic along with the incremental number of conservation treatments. This could mainly be due to the generated barium sulfate and calcium carbonate. They have fairly low solubility and are able to cling tightly to the gypsum crusts, making them more durable and allowing for better water resistance.

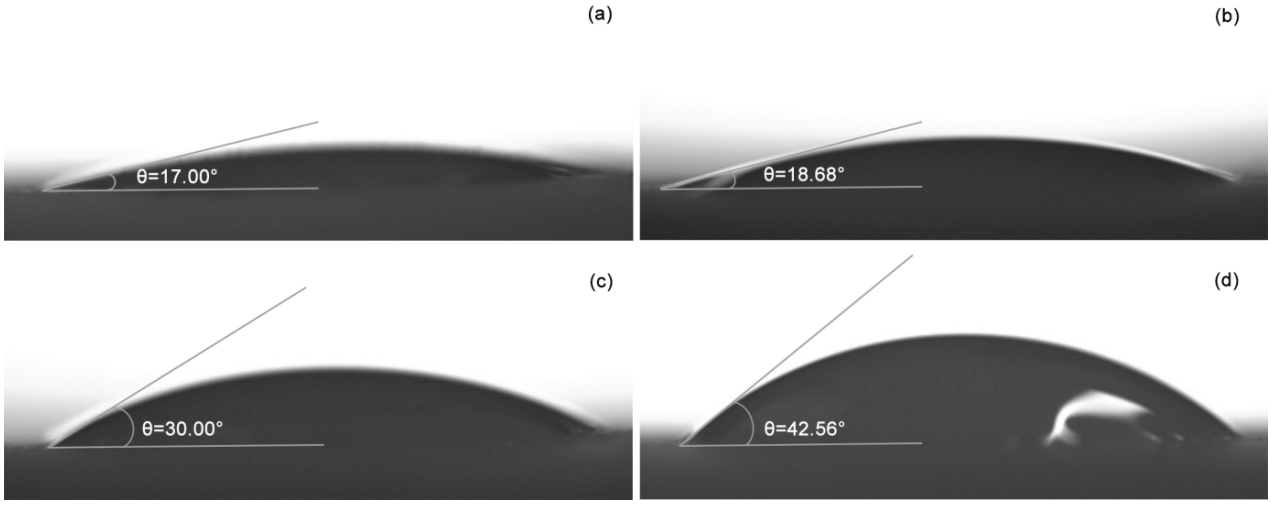

Figure 11. Wetting angles of the specimens with different treatment numbers, (**a**) blank specimen, (**b**) specimen after a single treatment, (**c**) specimen after two treatments, (**d**) specimen after three treatments.

The outcomes of the color differences of the specimens before and after treatment are shown in Table 2. According to the formula mentioned above, the color differences (ΔE*) of the treated specimens compared with the blank specimens were calculated. The results of the specimens with different treatment numbers are all varied in a range far below 5; this will not be recognized by the human eye [46]. It signifies that the "original appearance" of the specimen was almost unaffected after the introduction of the methanol solution of barium hydroxide-urea; this is of vital importance for cultural heritage objects.

Table 2. Color differences of the specimens before and after treatment.

Specimens with Different Treatment Numbers	L*	a*	b*	ΔL*	Δa*	Δb*	ΔE*
0 (blank)	38.98	0.99	3.90	-	-	-	-
1	39.14	0.88	3.34	0.16	−0.11	−0.56	0.59
2	38.65	0.92	3.28	−0.33	−0.07	−0.62	0.71
3	39.18	0.78	2.82	0.20	−0.21	−1.08	1.12

The results of the open porosity and capillary water absorption of the specimens are presented in Figures 12 and 13. The open porosity of the specimens decreased from about 40% to 34% after three treatments (Figure 12). This suggests that the specimens acquired denser and more compact structures after treatment, which is clearly shown in the SEM results. This could be mainly due to the adequate introduction of the methanol solution of barium hydroxide-urea. As a consequence of the formation of the inert protective barium calcium sulfate carbonate layer, the capillary water absorptions of the specimens reduced from about 30% to 23% (Figure 13). The extent of this variation is an evident change indeed. However, it is not unacceptable when compared with synthetic polymer film [47]. This is roughly consistent with the results obtained for the wetting angle: the hydrophilic nature of the primordial gypsum crust can be considered largely maintained, especially because the solubility of the specimens is significantly reduced.

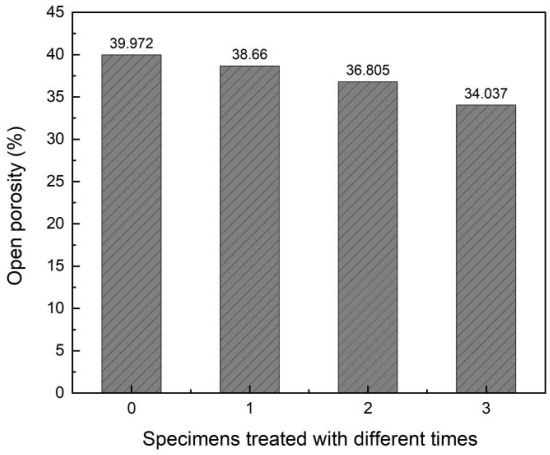

Figure 12. Open porosity of the specimens before and after treatment.

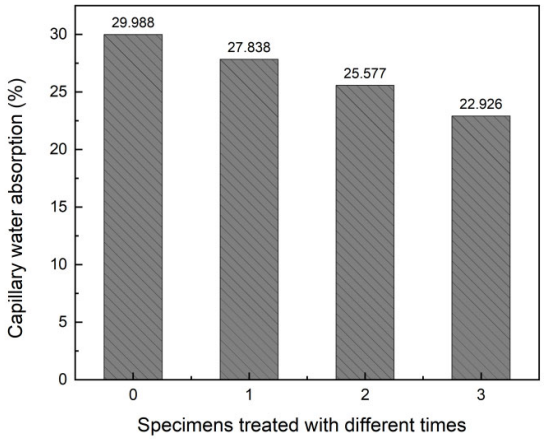

Figure 13. Capillary water absorption of the specimens before and after treatment.

The surface hardness of the specimens before and after treatment are shown in Figure 14. The average surface hardness of the blank specimens is about 69.1 HD, which increases to about 72.5 HD after three treatments. This is in accordance with the results of the SEM and the open porosity. After the introduction of the methanol solution of barium hydroxide-urea, the initial loose gypsum structure was wrapped rigidly by the producing barium sulfate and calcium carbonate. As a result, a denser structure emerged and eventually gave rise to an increase in the surface hardness.

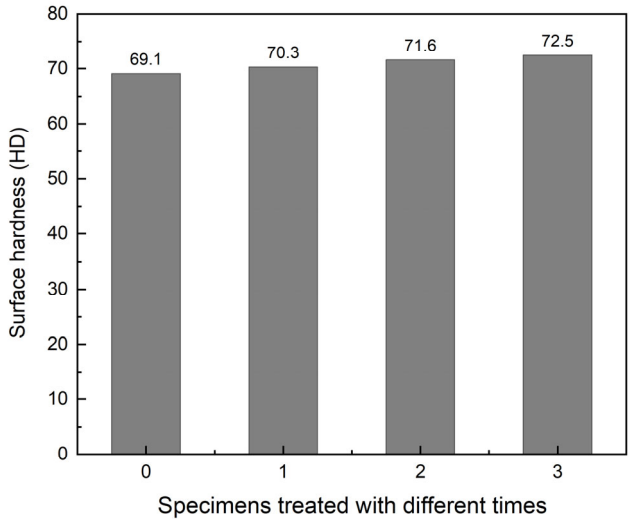

Figure 14. Surface hardness of the specimens before and after treatment.

4. Conclusions

Herein, an innovative route using a methanol solution of barium hydroxide-urea for the conservation of stone artifacts with gypsum weathering crusts was investigated. After the introduction of the barium hydroxide-urea methanol solution and water, in sequence, the barium sulfate and calcium carbonate layer were formed to provide prolonged protection for the brittle stone artifacts; this reaction can be completed within one week. Because of the low content of carbon dioxide in the natural atmosphere and the complete carbonization reaction difficulty that the internal substrate could face, the urea was added as a modifier into the methanol solution of barium hydroxide to provide a continuous source of carbonate ions. In addition, the existence of the urea did not affect the high solubility of the barium hydroxide in the methanol or the ability of the barium hydroxide methanol solution to penetrate deep into the substrate.

The conservation effect of the methanol solution of barium hydroxide-urea was satisfying. The conductivity and IC results reveal a clear increase in the water resistance ability of the treated specimens, which can be up to ten times stronger than the blank specimens. Meanwhile, the results of a larger surface hardness value indicate more solid structures of the surface gypsum crusts of the treated specimens. In addition, the results of the color difference, wetting angle, open porosity, and capillary water absorption denote that the inherent physical properties of the gypsum crust and original appearance were hardly altered. These positive results show that the methanol solution of barium hydroxide-urea could have great potential in the conservation of stone artifacts with gypsum weathering crusts.

However, there are still limitations to this method that can be further studied. It was noticed that the urea could produce carbon dioxide as well as ammonia, which is an irritant. Thus, how to reduce the irritation of ammonia still needs further investigation. In addition, the use of the methanol solvent could be detrimental to human health. Hence, there is a need to find ways to diminish this harm. We hope that through a continuous investigation, there will be more exciting findings about this novel conservation method.

Author Contributions: Conceptualization, F.Y.; Data curation, R.L., L.H., T.L., Y.L. and X.C.; Investigation, R.L., L.H., Y.L., T.L. and K.Z.; Methodology, F.Y.; Writing—original draft, R.L.; Writing—review & editing, R.L. and Y.L. All authors have read and agreed to the published version of the manuscript.

Funding: This research was funded by the National Natural Science Foundation of China (B0501 21975202, 52108031); the Collaborative Innovation Team Foundation of University in Gansu Province (2017C-20); 111 project (D18004) and the Key R&D Program in Shaanxi Province (2020SF-363).

Institutional Review Board Statement: Not applicable.

Informed Consent Statement: Not applicable.

Data Availability Statement: Not applicable.

Conflicts of Interest: The authors declare no conflict of interest.

References

1. Bozdağ, A.; Ince, I.; Bozdağ, A.; Hatır, M.E.; Tosunlar, M.B.; Korkanç, M. An assessment of deterioration in cultural heritage: The unique case of Eflatunpınar Hittite Water Monument in Konya, Turkey. *Bull. Eng. Geol. Environ.* **2020**, *79*, 1185–1197. https://doi.org/10.1007/s10064-019-01617-9.
2. Camuffo, D. Deterioration Processes of Historical Monuments. In *Studies Environmental Science*; Schneider, T., Ed.; Elsevier: Amsterdam, The Netherlands, 1986; Volume 30, pp. 189–221. https://doi.org/10.1016/s0166-1116(08)70884-7.
3. Charola, A.E.; Ware, R. Acid deposition and the deterioration of stone: A brief review of a broad topic. *Geol. Soc. Lond. Spec. Publ.* **2002**, *205*, 393–406. https://doi.org/10.1144/gsl.sp.2002.205.01.28.
4. Ausset, P.; Lefèvre, R.A.; Del Monte, M. Early mechanisms of development of sulphated black crusts on carbonate stone. In *Proceedings of the 9th International Congress on Deterioration and Conservation of Stone*; Fassina, V., Ed.; Elsevier Science B.V.: Amsterdam, The Netherlands, 2000; pp. 329–337. https://doi.org/10.1016/b978-044450517-0/50115-x.
5. Dean, J.A. *Lange's Handbook of Chemistry*; Wei, J.F., Ed.; Science Press: Beijing, China, 2003.
6. Kramar, S.; Urosevic, M.; Pristacz, H.; Mirtič, B. Assessment of limestone deterioration due to salt formation by micro-Raman spectroscopy: Application to architectural heritage. *J. Raman Spectrosc.* **2010**, *41*, 1441–1448. https://doi.org/10.1002/jrs.2700.
7. Fronteau, G.; Schneider-Thomachot, C.; Chopin, E.; Barbin, V.; Mouze, D.; Pascal, A. Black-crust growth and interaction with underlying limestone microfacies. *Geol. Soc. Lond. Speec. Publ.* **2010**, *333*, 25–34. https://doi.org/10.1144/sp333.3.
8. Zanini, A.; Trafeli, V.; Bartoli, L. The laser as a tool for the cleaning of Cultural Heritage. *IOP Conf. Ser. Mater. Sci. Eng.* **2018**, *364*, 012078. https://doi.org/10.1088/1757-899x/364/1/012078.
9. Gioventù, E.; Lorenzi, P. Bio-Removal of Black Crust from Marble Surface: Comparison with Traditional Methodologies and Application on a Sculpture from the Florence's English Cemetery. *Procedia Chem.* **2013**, *8*, 123–129. https://doi.org/10.1016/j.proche.2013.03.017.
10. Pozo-Antonio, J.; Rivas, T.; López, A.; Fiorucci, M.; Ramil, A. Effectiveness of granite cleaning procedures in cultural heritage: A review. *Sci. Total Environ.* **2016**, *571*, 1017–1028. https://doi.org/10.1016/j.scitotenv.2016.07.090.
11. Liu, Y.; Dong, T.; Zhang, K.; Yang, F.; Wang, L. Preliminary Study of the Targeted Cleaning of an Artificial Gypsum Layer on White Marble. *Coatings* **2021**, *11*, 37. https://doi.org/10.3390/coatings11010037.
12. Zezza, F. The Monument Stone: An Eternal Link of Past Civilizations. In 10th International Symposium on the Conservation of Monuments in the Mediterranean Basin: Natural and Anthropogenic Hazards and Sustainable Preservation; Koui, M., Zezza, F., Kouis, D., Eds.; Springer International Publishing: Cham, Switzerland, 2018; pp. 17–28. https://doi.org/10.1007/978-3-319-78093-1_3.
13. Artesani, A.; Di Turo, F.; Zucchelli, M.; Traviglia, A. Recent Advances in Protective Coatings for Cultural Heritage—An Overview. *Coatings* **2020**, *10*, 217. https://doi.org/10.3390/coatings10030217.
14. Zhang, H.; Liu, Q.; Liu, T.; Zhang, B. The preservation damage of hydrophobic polymer coating materials in conservation of stone relics. *Prog. Org. Coat.* **2013**, *76*, 1127–1134. https://doi.org/10.1016/j.porgcoat.2013.03.018.
15. Frigione, M.; Lettieri, M. Novel Attribute of Organic–Inorganic Hybrid Coatings for Protection and Preservation of Materials (Stone and Wood) Belonging to Cultural Heritage. *Coatings* **2018**, *8*, 319. https://doi.org/10.3390/coatings8090319.
16. Li, W.; Lin, J.; Zhao, Y.; Pan, Z. The Adverse Effects of TiO_2 Photocatalycity on Paraloid B72 Hybrid Stone Relics Protective Coating Aging Behaviors under UV Irradiation. *Polymers* **2021**, *13*, 262. https://doi.org/10.3390/polym13020262.
17. Hansen, E.F.; Doehne, E.; Fidler, J.M.; Larson, J.D.; Martin, B.R.; Matteini, M.; Rodriguez-Navarro, C.; Pardo, E.S.; Price, C.; De Tagle, A.; et al. A review of selected inorganic consolidants and protective treatments for porous calcareous materials. *Stud. Conserv.* **2003**, *48*, 13–25. https://doi.org/10.1179/sic.2003.48.supplement-1.13.
18. Drdácký, M.; Slížková, Z. Calcium hydroxide based consolidation of lime mortars and stone. In Proceedings of the International Symposium 'Stone Consolidation in Cultural Heritage', Lisbon, Portugal, 23–25 March 2022; pp. 299–308. Available online: https://www.researchgate.net/publication/313064616 (accessed on 31 October 2022).
19. Hall, L.R.; Matero, F.G. Considerations on Complex Sequential Treatments of Gypsum Crusts: The Carrara Marble Capitals of the Philadelphia Merchants' Exchange. *J. Am. Inst. Conserv.* **2011**, *50*, 123–148. https://doi.org/10.1179/019713611804480917.

20. Sayre, E.V. Direct Deposition of Barium Sulfate from Homogeneous Solution within Porous Stone. *Stud. Conserv.* **1971**, *16*, 115–117. https://doi.org/10.1080/00393630.1971.11673770.
21. Baglioni, P.; Chelazzi, D.; Giorgi, R. *Nanotechnologies in the Conservation of Cultural Heritage: A Compendium of Materials and Techniques*; Baglioni, P., Chelazzi, D., Giorgi, R., Eds.; Springer: Amsterdam, The Netherlands, 2015; pp. 15–59. https://doi.org/10.1007/978-94-017-9303-2_2.
22. Magrini, D.; Bartolozzi, G.; Bracci, S.; Carlesi, S.; Cucci, C.; Picollo, M. Evaluation of the efficacy and durability of the "barium hydroxide method" after 40 years. Multi-analytical survey on the Crocifissione by Beato Angelico. *J. Cult. Herit.* **2020**, *45*, 362–369. https://doi.org/10.1016/j.culher.2020.04.006.
23. Toniolo, L.; Colombo, C.; Realini, M.; Peraio, A.; Positano, M. Evaluation of barium hydroxide treatment efficacy on a dolomitic marble. *Ann. Chim.* **2001**, *91*, 813–821.
24. Salvadori, B.; Errico, V.; Mauro, M.; Melnik, E.; Dei, L. Evaluation of Gypsum and Calcium Oxalates in Deteriorated Mural Paintings by Quantitative FTIR Spectroscopy. *Spectrosc. Lett.* **2003**, *36*, 501–513. https://doi.org/10.1081/sl-120026615.
25. Pastuović, Ž.; Fazinić, S.; Jakšić, M.; Krstić, D.; Mudronja, D. The use of the RBI nuclear microprobe in conservation process studies of a church portal. *Nucl. Instrum. Methods Phys. Res. Sect. B Beam Interact. Mater. Atoms* **2005**, *231*, 546–552. https://doi.org/10.1016/j.nimb.2005.01.115.
26. Sassoni, E.; Graziani, G.; Franzoni, E.; Scherer, G.W. Conversion of calcium sulfate dihydrate into calcium phosphates as a route for conservation of gypsum stuccoes and sulfated marble. *Constr. Build. Mater.* **2018**, *170*, 290–301. https://doi.org/10.1016/j.conbuildmat.2018.03.075.
27. Chelazzi, D.; Poggi, G.; Jaidar, Y.; Toccafondi, N.; Giorgi, R.; Baglioni, P. Hydroxide nanoparticles for cultural heritage: Consolidation and protection of wall paintings and carbonate materials. *J. Colloid Interface Sci.* **2013**, *392*, 42–49. https://doi.org/10.1016/j.jcis.2012.09.069.
28. Saoud, K.M.; Ibala, I.; El Ladki, D.; Ezzeldeen, O.; Saeed, S. *Digital Heritage. Progress in Cultural Heritage: Documentation, Preservation, and Protection*; Ioannides, M., Ed.; Springer International Publishing: Berlin/Heidelberg, Germany, 2014; pp. 342–352. https://doi.org/10.1007/978-3-319-13695-0_33.
29. Lu, R.; Wang, L.; Liu, Y.; Yang, F.; Yang, L.; Wang, L.; Gao, X. Conservation of surface gypsification stone relics using methanol solution of barium hydroxide as a novel treating agent. *Appl. Phys. A* **2021**, *128*, 37. https://doi.org/10.1007/s00339-021-05185-2.
30. Durán-Suárez, J.; García-Beltrán, A.; Rodríguez-Gordillo, J. Colorimetric cataloguing of stone materials (biocalcarenite) and evaluation of the chromatic effects of different restoring agents. *Sci. Total Environ.* **1995**, *167*, 171–180. https://doi.org/10.1016/0048-9697(95)04578-o.
31. Camuffo, D.; Del Monte, M.; Sabbioni, C.; Vittori, O. Wetting, deterioration and visual features of stone surfaces in an urban area. *Atmos. Environ.* **1982**, *16*, 2253–2259. https://doi.org/10.1016/0004-6981(82)90296-7.
32. Cabañas, M.V.; Rodríguez-Lorenzo, L.M.; Vallet-Regí, M. Setting Behavior and in Vitro Bioactivity of Hydroxyapatite/Calcium Sulfate Cements. *Chem. Mater.* **2002**, *14*, 3550–3555. https://doi.org/10.1021/cm021121w.
33. Favaro, M.; Tomasin, P.; Ossola, F.; Vigato, P.A. A novel approach to consolidation of historical limestone: The calcium alkoxides. *Appl. Organomet. Chem.* **2008**, *22*, 698–704. https://doi.org/10.1002/aoc.1462.
34. Rodriguez-Navarro, C.; Suzuki, A.; Ruiz-Agudo, E. Alcohol dispersions of calcium hydroxide nanoparticles for stone conservation. *Langmuir* **2013**, *29*, 11457–11470. https://doi.org/10.1021/la4017728.
35. Kroftová, K.; Škoda, D.; Kuřitka, I.; Kubát, J. Technology of preparation of barium and magnesium hydroxide nanodispersion and possibilities of their use in monument care. *Contem. Mater. Technol. Civ. Eng.* **2018**, *2019*, 21–23. https://doi.org/10.14311/app.2019.21.0021.
36. Starikova, Z.A.; Kessler, V.G.; Turova, N.Y.; Dantsker, I.A.; Bobyljov, A.P.; Mitiaev, A.S. Interaction of barium oxide and hydroxide with methanol: X-ray single crystal study of Ba(OH)2 methanol solvates. *Polyhedron* **2006**, *25*, 2401–2406. https://doi.org/10.1016/j.poly.2006.02.014.
37. Hussain, R.; Devi, R.R.; Maji, T.K. Controlled release of urea from chitosan microspheres prepared by emulsification and cross-linking method. *Iran. Polym. J.* **2012**, *21*, 473–479. https://doi.org/10.1007/s13726-012-0051-0.
38. Chakrabarty, D.; Mahapatra, S. Aragonite crystals with unconventional morphologies. *J. Mater. Chem.* **1999**, *9*, 2953–2957. https://doi.org/10.1039/a905407c.
39. Al Omari, M.M.H.; Rashid, I.S.; Qinna, N.A.; Jaber, A.M.; Badwan, A.A. Calcium Carbonate. In *Profiles of Drug Substances, Excipients and Related Methodology*; Elsevier: Amsterdam, The Netherlands, 2016; Volume 41, pp. 31–132.
40. Zuena, M.; Zendri, E.; Costa, D.; Delgado-Rodrigues, J.; El Habra, N.; Tomasin, P. Calcium Ethoxide as Consolidant for Porous Limestones: Influence of the Solvent. *Coatings* **2019**, *9*, 83. https://doi.org/10.3390/coatings9020083.
41. Ramaswamy, V.; Vimalathithan, R.M.; Ponnusamy, V. Synthesis and characterization of BaSO4 nano particles using micro emulsion technique. *Adv. Appl. Sci. Res.* **2010**, *1*, 197–204.
42. Tomasin, P.; Mondin, G.; Zuena, M.; El Habra, N.; Nodari, L.; Moretto, L.M. Calcium alkoxides for stone consolidation: Investigating the carbonation process. *Powder Technol.* **2019**, *344*, 260–269. https://doi.org/10.1016/j.powtec.2018.12.050.
43. Wilcox, L.V. Electrical Conductivity. *J. AWWA* **1950**, *42*, 775–776. https://doi.org/10.1002/j.1551-8833.1950.tb18892.x.
44. Sassoni, E.; Graziani, G.; Franzoni, E. An innovative phosphate-based consolidant for limestone. Part 1: Effectiveness and compatibility in comparison with ethyl silicate. *Constr. Build. Mater.* **2016**, *102*, 918–930. https://doi.org/10.1016/j.conbuildmat.2015.04.026.

45. Liu, Q.; Zhang, B.J. Assessment of Damage from Organic Protective Coating Treatments to Historic Stone Buildings and Sculptures. *Appl. Mech. Mater.* **2010**, *44–47*, 610–613. https://doi.org/10.4028/www.scientific.net/amm.44-47.610.
46. García, O.; Malaga, K. Definition of the procedure to determine the suitability and durability of an anti-graffiti product for application on cultural heritage porous materials. *J. Cult. Herit.* **2012**, *13*, 77–82. https://doi.org/10.1016/j.culher.2011.07.004.
47. Tsakalof, A.; Manoudis, P.; Karapanagiotis, I.; Chryssoulakis, I.; Panayiotou, C. Assessment of synthetic polymeric coatings for the protection and preservation of stone monuments. *J. Cult. Herit.* **2007**, *8*, 69–72. https://doi.org/10.1016/j.culher.2006.06.007.